Published in final edited form as:
Nat Immunol. 2013 February ; 14(2): 152–161. doi:10.1038/ni.2496.

PD-1 controls Lymph Node and Blood T Follicular Regulatory Cells

Peter T. Sage[1,2], **Loise M. Francisco**[1,3], **Christopher V. Carman**[2], and **Arlene H. Sharpe**[1,3,*]

[1]Department of Microbiology and Immunobiology, Harvard Medical School, Boston, MA, 02115

[2]Department of Medicine, Beth Israel Deaconess Medical Center, Boston, MA, 02215

[3]Department of Pathology, Brigham and Women's Hospital, Boston, MA, 02115

Abstract

Newly defined $CD4^+CXCR5^+FoxP3^+$ T Follicular Regulatory (TFR) cells inhibit $CD4^+CXCR5^+FoxP3^-$ T Follicular Helper (TFH)-mediated humoral immunity. Although PD-1 is expressed by both cell types, the role of this inhibitory receptor on TFR differentiation is unknown. Here we show that PD-1/PD-L1 deficient mice have increased lymph node TFR cells, which have enhanced suppressive capacity. We also find substantial populations of TFR cells in mouse blood, and demonstrate that blood TFR cells home to lymph nodes and potently inhibit TFH cells *in vivo*. Blood TFR cells require CD28 and ICOS signaling, but are inhibited by PD-1/PD-L1. These findings reveal novel mechanisms by which the PD-1 pathway regulates antibody production and helps to reconcile inconsistencies surrounding the role of this pathway in humoral immunity.

Follicular helper T cells (TFH) are a recently defined subset of CD4 T cells that are essential for helping cognate B cells form and maintain the germinal center (GC) reaction, and for development of humoral immune responses. These cells are universally defined by expression of the chemokine receptor CXCR5, which directs them to the B cell follicles via gradients of the chemokine CXCL13 [1]. TFH cells also express the transcription factor *Bcl6* (which represses Blimp-1/*Prdm*1) and high levels of the costimulatory receptor ICOS, which are both critical for their differentiation and maintenance [1–4]. In addition, TFH cells secrete large amounts of IL-21, which aids in GC formation, isotype switching and plasma cell formation [5]. In humans and mice functionally similar TFH cells can be found in secondary lymphoid organs. Significantly, $CXCR5^+$ TFH cells are also present in peripheral blood and seen at elevated levels in individuals with autoantibodies, including systemic lupus erythematosis, myasthenia gravis and juvenile dermatomyositis patients. However, the function of these circulating TFH remains unclear [6–9].

TFH cells also express high levels of programmed death (PD) 1 receptor (CD279). Signaling through PD-1 attenuates TCR signals and inhibits T cell expansion, cytokine production and cytolytic function. In addition, PD-1 promotes the development of induced regulatory T (iTreg) cells from naïve lymphocytes [10–14]. PD-1 has two ligands, PD-L1 (B7-H1) and PD-L2 (B7-DC). PD-L1 is more widely expressed than PD-L2, but PD-L1 and PD-L2 both can be expressed on GC B cells and dendritic cells [15]. Perturbation studies suggest critical roles for this pathway in regulating humoral immune responses. However, there are conflicting reports as to the function of the PD-1 pathway in controlling humoral immunity. Some

*Correspondence: Arlene_Sharpe@hms.harvard.edu.

studies have found that humoral responses are attenuated [16–18], while others have seen that humoral responses are heightened [19, 20] when PD-1:PD-L interactions are prevented.

PD-1 also is found on a newly defined subset of $CD4^+CXCR5^+$ cells called T follicular regulatory (TFR) cells, which are positive for the transcription factors FoxP3, *Bcl6* and *Prdm1*/Blimp1 and function to inhibit the germinal center response [21–23]. These cells originate from natural regulatory T cell precursors, but express similar levels of ICOS, CXCR5 and PD-1 as TFH cells. Since ICOS, CXCR5 and PD-1 have been widely used to identify and purify 'TFH cells', it seems likely that the inability to define clear functions for PD-1 in GC responses derives from experimental systems containing mixtures of stimulatory TFH cells and inhibitory TFR cells. Separate analyses of the function of PD-1 on TFH and TFR cells are needed to elucidate how PD-1 controls humoral immunity and to gain insight into the individual roles of TFR cells and TFH cells in regulating antibody production.

Here we demonstrate that PD-1:PD-L1 interactions inhibit TFR, but not TFH, cell numbers in lymph nodes. PD-1 deficient mice have increased numbers of lymph node TFR cells compared to wild type mice. PD-1 deficient lymph node TFR cells have enhanced ability to suppress activation of naïve T cells, as well as antibody production *in vitro*. In addition, we show for the first time that TFR cells are present in the peripheral blood of mice, and that these circulating cells can potently regulate humoral immune responses *in vivo*. Using transfer approaches, we demonstrate that blood TFH cells can promote antibody production, while blood TFR cells can strongly inhibit antibody production *in vivo*. We further show that the PD-1 pathway inhibits blood TFR cell function and PD-1 deficient blood TFR cells have enhanced suppressive capacity *in vivo*. Taken together, our studies reveal a new immunoregulatory role for the PD-1:PD-L1 pathway in limiting TFR cell differentiation and function, and further demonstrate the dynamic control of humoral immune responses by migration of TFR cells from the circulation into lymph nodes to control antibody production *in vivo.*

Results

PD-1 Controls T Follicular Regulatory Cells

To analyze the role of PD-1 in controlling T follicular regulatory (TFR) cells, we first compared PD-1 expression on CD4 T cell subsets in draining lymph nodes (dLN) of WT C57BL/6 mice subcutaneously immunized with myelin oligodendrocyte glycoprotein (MOG) peptide 35–55 emulsified in CFA (from hereon simply referred to as "MOG/CFA"), an immunization that breaks tolerance and also results in effective TFH cell generation [24]. TFR cells were defined as $CD4^+ICOS^+CXCR5^+FoxP3^+CD19^-$, a gating strategy that separates TFR cells from $CD4^+ICOS^+CXCR5^+FoxP3^-CD19^-$ TFH cells, the cell type that was until recently thought to solely comprise the $CD4^+CXCR5^+$ gate (Figure 1a). TFH cells showed higher expression of PD-1 compared to $ICOS^+CXCR5^-$ effector-like cells and $ICOS^-CXCR5^-$ naïve (referred to as naïve) cells in the draining lymph node on day 7 after immunization. Strikingly, TFR cells had even higher PD-1 expression when compared to the other CD4 T cell subsets examined, including TFH cells (Figure 1b).

To determine the functional significance of PD-1 expression on TFR cells, we immunized WT and PD-$1^{-/-}$ mice and analyzed TFR cells 7 days later. The percentage of TFR cells contained within the $CD4^+FoxP3^+$ gate was about 4 percent in WT lymph nodes and less than 1 percent of all CD4 T cells. In marked contrast, the percentage of TFR cells in PD-$1^{-/-}$ mice was about 10 percent of the $CD4^+FoxP3^+$ gate and greater than 2 percent of all CD4 T cells (Figure 1c–d). Because total numbers of CD4 T cells are typically about two fold higher in the lymph nodes of PD-1 deficient animals, a two-fold increase in TFR cell

frequency translates into a ~4-fold increase in absolute numbers of TFR cells (data not shown). When expressed as a percentage of all $CD4^+ICOS^+CXCR5^+$ cells (and therefore the percentage of CD4 T cells that respond to CXCL13 and migrate to the B cell zone), PD-$1^{-/-}$ TFR cells comprised half of this population, whereas WT TFR cells comprised only about 20 percent (Figure 1d). The dramatic increase in the percentage of TFR cells in PD-$1^{-/-}$ mice also was observed when other classical B cell antigens, such as 4-hydroxy-3-nitrophenylacetyl hapten conjugated to ovalbumin (NP-OVA), were used (Figure S1). We did not find a significant difference in the percentage of $FoxP3^-$ TFH (from hereon called "TFH") cells when expressed as a percentage of all CD4 T cells in WT and PD-$1^{-/-}$ mice on day 7 post immunization (Figure 1e).

Since PD-1 can be expressed by a number of hematopoietic cell types including T cells, B cells, macrophages and some dendritic cells [15], we next investigated whether PD-1 regulates TFR cells directly by controlling their generation from $FoxP3^+$ T regulatory cells (Treg). To track the fate of $FoxP3^+$ cells following transfer into WT mouse recipients, we used antigen-specific $FoxP3^+$ T cells from TCR transgenic mice for these studies. We sorted $FoxP3^+$ Tregs from WT or PD-$1^{-/-}$ 2D2 (MOG–specific) TCR transgenic FoxP3 GFP reporter mice and transferred 2×10^5 2D2 WT or PD-$1^{-/-}$ $CD4^+CXCR5^-FoxP3^+$ cells into WT recipient mice. We immunized these recipients with MOG/CFA and analyzed cells in the draining lymph node seven days later (Figure 1f). There were a greater percentage (Figure 1h) and absolute number (Figure 1i) of 2D2 PD-$1^{-/-}$ Tregs upregulating CXCR5 and thus differentiating into TFR cells, compared to 2D2 WT Tregs. The increased percentage of PD-$1^{-/-}$ TFR cells in the immunized transfer recipients was similar, but less pronounced, than the increased percentage in TFR cells seen in immunized intact PD-1 deficient mice (Figure 1d, h). These results demonstrate that PD-1 controls differentiation of $FoxP3^+$ Tregs into TFR cells.

Since CD25 (the alpha chain of the IL-2 receptor) is frequently used as a marker for Tregs, we next compared CD25 expression on WT and PD-$1^{-/-}$ TFR cells directly *ex vivo* (Figure 2a). PD-$1^{-/-}$ TFR cells expressed less CD25 than WT TFR cells (Figure 2b). The attenuated CD25 expression in PD-1 deficient TFR cells is not likely due to decreased activation because the expression of the early activation marker CD69 was virtually identical on WT and PD-$1^{-/-}$ TFR cells (Figure 2c). To compare the proportion of WT and PD-$1^{-/-}$ TFR cells proliferating at day 7 post immunization, we examined Ki67 expression, a marker widely used to identify cells that are actively dividing. WT $ICOS^+$ $CXCR5^-$ effectors, TFH and TFR gated cells had high expression of Ki67. In contrast, the WT $CXCR5^-ICOS^-$ "naïve" cells, lacking CD69 and CD25 expression, had no Ki67 staining consistent with their designation as naïve (Figure 2d). WT TFR cells expressed significantly higher levels of Ki67 compared to PD-$1^{-/-}$ TFR cells, suggesting that the increased numbers of TFR cells in PD-1 deficient animals reflect increased differentiation, and not maintenance, of TFR cells. Ki67 expression was similarly greater in WT $ICOS^+$ effectors and TFH cells compared to PD-$1^{-/-}$ $ICOS^+$ $CXCR5^-$ effectors and TFH cells. This points to an overall decrease in cell cycling in PD-$1^{-/-}$ effector cells at 7 days after immunization. Other Treg markers such as CD103 and GITR were not altered on TFR cells in PD-1 deficient mice (Figure S2). Additionally, there was low, but significant expression of PD-L1 on WT and PD-$1^{-/-}$ TFR cells (Figure S2). Together, these data indicate that PD-1 is important in regulating numbers of TFR cells *in vivo*.

PD-1 Deficient TFR cells are Capable of Homing to Germinal Centers

We next compared the capacity of TFR cells from WT and PD-1 deficient animals to enter the germinal center (GC) in order to inhibit the GC response. First, we evaluated GC formation in lymph node sections harvested 7 days after MOG/CFA immunization. GCs were identified by the presence of PNA/GL7 positively stained and IgD negatively stained B

cell zones (Figure 3a). These GCs were determined to be active, based on robust expression of the cell cycle marker Ki67 (Figure 3b). Similar to previous reports [21, 22], $CD4^+FoxP3^+$ TFR cells could be found within GCs of immunized mice (Figure 3c). The FoxP3 protein within the TFR cells was judged to be largely nuclear based on its co-localization with the DAPI staining (Figure 3d).

We then investigated whether the phenotypically distinct TFR cells from PD-1 deficient mice were able to migrate to GCs similarly to WT TFR cells, because PD-1 blockade can prolong the TCR stop signal and decrease T cell migration [25]. We immunized WT and PD-1 deficient mice with MOG/CFA and 7 days later analyzed lymph node sections for IgD, GL7 and FoxP3 expression (Figure 3e). Although the average germinal center area (Figure 3f) and numbers of germinal centers per lymph node (data not shown) were equivalent in WT and PD-$1^{-/-}$ mice, there were slightly more $FoxP3^+$ cells (and therefore TFR cells) located within the GC borders in PD-$1^{-/-}$ mice as in WT mice (Figure 3g). However, since this increase is proportional to the larger numbers of TFR cells in PD-1 deficient mice determined by flow cytometry, these data demonstrate that PD-1 deficient TFR cells are not defective in homing to GCs and can enter the GC similarly to WT TFR cells.

The relative location of $FoxP3^+$ TFR cells within the GC did not differ significantly between WT and PD-$1^{-/-}$ TFR cells (Figure 3h). In both WT and PD-$1^{-/-}$ mice the $FoxP3^+$ cells tended to reside close to the GC border, with more than half of the $FoxP3^+$ nuclei being positioned within 10μm of the border. Furthermore, when CXCR5 fluorescence was quantified by flow cytometry in TFR cells, there was similar CXCR5 expression on TFR cells in the WT and PD-$1^{-/-}$ mice, indicating similar potential for these cells to respond to chemokine cues to migrate to GCs (Figure 3i). Taken together, these data indicate that TFR cells are increased in lymph nodes of immunized PD-$1^{-/-}$ mice, and these PD-$1^{-/-}$ TFR cells are capable of migrating into GCs to regulate B cell responses.

PD-1 deficient TFR cells More Potently Inhibit T Cell Activation

We next compared the function of TFR cells from WT and PD-$1^{-/-}$ mice. TFR cells express higher levels of GITR on the cell surface than do TFH cells, which allows for separation of the TFH and TFR cells in a similar manner to intracellular staining for FoxP3 (Figure 4a). For functional studies, we sorted TFR cells from immunized mice by taking the lymph node $CD4^+ICOS^+CXCR5^+CD19^-GITR^+$ population as TFR cells and the $CD4^+ICOS^+CXCR5^+CD19^-GITR^-$ population as TFH cells (Figure 4b). Sorting in this fashion shows robust mRNA for FoxP3 in the $GITR^+$ (TFR) population, but essentially no FoxP3 mRNA in the $GITR^-$ (TFH) population, validating the use of this gating strategy to isolate TFR and TFH cells for functional assays. Furthermore, this sorting strategy can be used to compare WT and PD-1 deficient TFR cells since GITR expression is identical on WT and PD-1 deficient TFR cells (Figure S3).

TFR cells express high Blimp1/*Prdm1* and moderate levels of Bcl6 [21]. Bcl6 and Blimp1 reciprocally modulate each other [2]; Bcl6 inhibition of Blimp1 is essential for maintenance of the TFH phenotype, whereas Blimp1 is important in Treg homeostasis in general [26, 27]. Since relative expression of Bcl6 and Blimp1 determines function of TFH subsets, we compared Bcl6 expression in TFR cells from WT and PD-$1^{-/-}$ mice using flow cytometry to analyze intracellular Bcl6 expression at the protein level. Although TFR cells expressed less Bcl6 at the protein level than TFH cells, WT and PD-$1^{-/-}$ TFR had similar Bcl6 levels (Figure 4c). We next compared the expression of Blimp1 (encoded by *Prdm1*) on TFR cells from WT and PD-$1^{-/-}$ mice. At the mRNA level, we did not find any consistent differences in Blimp1/*Prdm1* expression between WT and PD-$1^{-/-}$ TFR cells (Figure 4d). Since FoxP3 can directly interact with and negatively regulate the function of Rorγt [28], we also examined *Rorc* (which encodes Rorγt) in WT and PD-$1^{-/-}$ TFR cells. *Rorc* mRNA levels were lower

in TFR cells compared to TFH cells, but *Rorc* expression was increased in PD-1$^{-/-}$ TFR cells relative to WT TFR cells (Figure 4e). In addition, we compared expression of the transcription factor IRF4 in WT and PD-1$^{-/-}$ TFR cells, since Blimp1 and IRF4 synergistically control the differentiation and effector functions of regulatory T cells [26]. We found an increase in *IRF4* mRNA in PD-1$^{-/-}$ TFR cells compared to WT TFR cells (Figure 4f).

IRF4 is essential for the suppressive capacity of regulatory T cells [26]. To determine if increased IRF4 mRNA in PD-1$^{-/-}$ TFR cells translates into an increase in suppression of naïve T cell proliferation, we set up an *in vitro* suppression assay in which we cultured sorted WT GL7^{-} B cells, CFSE labeled WT naïve CD4^{+}CD62L^{+}FoxP3^{-} responder T cells, and either WT or PD-1$^{-/-}$ TFR cells sorted from mice immunized with MOG/CFA together with anti-CD3 and anti-IgM (Figure 4g). The responder T cells highly upregulated CD69 after 3 days of culture with WT B cells. However, when WT TFR cells were added in a 1:1:1 ratio, the CD69 expression on the responder T cells was much lower, consistent with the function of TFR cells in suppressing T cell activation (Figure 4h). CD69 upregulation was inhibited to an even greater extent in responder T cells that were cultured with PD-1$^{-/-}$ TFR cells. Moreover, PD-1$^{-/-}$ TFR attenuated the proliferation of responder T cells (Figure 4i), in contrast to WT TFR cells, which did not inhibit the proliferation of responder T cells during the day 3 culture period.

Although TFR cells are thought to inhibit the germinal response *in vivo,* it is unclear whether TFR cells directly inhibit T cell differentiation, TFH cell function, B cell activation or all three. To assess the capability of TFR cells to suppress B cell antibody production *in vitro*, we cultured WT GL7^{-} B cells with WT FoxP3^{-} TFH cells for 6 days in the presence or absence of TFR cells, anti-IgM and anti-CD3 (Figure 4j). WT B cells produced large amounts of IgG when cultured with WT FoxP3^{-} TFH cells plus anti-IgM and anti-CD3 (Figure 4k). No significant IgG was present when CD4^{+}FoxP3^{-} naïve T cells were used in these experiments (Figure 4l). When TFR cells were added to the wells along with TFH cells, almost no IgG was produced. The TFR-mediated suppression was not due to sequestering of anti-CD3 because there was equally good suppression at the two doses of anti-CD3 tested (Figure 4k), and the anti-CD3 could still be found on the surface of the TFH cells at the end of the suppression assay (Figure S4). PD-1$^{-/-}$ TFR cells suppressed IgG production more than WT TFR cells at both a 1:1 (Figure 4l) and a 1:5 (Figure 4m) TFR:TFH ratio, with PD-1 deficient TFR cells resulting in a 50% greater reduction in IgG production compared to WT TFR cells. Taken together, these data demonstrate not only that are there increased TFR cells in PD-1$^{-/-}$ mice, but that these PD-1$^{-/-}$ TFR cells have increased suppressive capacity.

PD-1 Controls Blood T Follicular Regulatory Cells

One possible explanation for the increase in TFR cells in lymph nodes of immunized PD-1 deficient mice is that PD-1$^{-/-}$ TFR cells are unable to exit the lymph node. Studies have demonstrated that functional TFH cells can be found in the blood of humans as well as mice [6, 7, 9], but whether TFR cells circulate in the blood of humans or mice is not yet known. Strikingly, we found a significant population of TFH cells, as well as a smaller population of TFR cells, in the blood of WT mice immunized with MOG/CFA (Figure 5a–b). When we compared the kinetics of TFH and TFR cell expansion in the lymph node and blood of mice following MOG/CFA immunization, we found that both TFR and TFH cells increase in the draining lymph node of WT immunized mice over a 10 day period, and that TFH cells, but not TFR cells, increase substantially by percentage in the blood over this time (Figure 5b). Thus, without antigenic stimulus, the blood TFR:TFH ratio is fairly high (sometimes greater than 1:1) but upon addition of a stimulus, blood TFH cells expand more than blood TFR cells so that the TFR:TFH ratio is about 1:5. To investigate whether WT blood TFH and

TFR cells are quiescent or are actively in cell cycle, we compared Ki67 expression in draining lymph node and blood TFH and TFR cells 7 days after immunization. TFH cells from the draining lymph node had higher Ki67 expression than those found in the blood (Figure 5c). Blood TFH and TFR and draining lymph node TFR cells expressed similar levels of Ki67.

Next we investigated whether TFR cells in the blood were inhibited to the same degree by PD-1 signaling as lymph node TFR cells. We immunized WT and PD-$1^{-/-}$ mice with MOG/CFA and 7 days later analyzed the blood for TFH and TFR cells. In WT mice ~2–3 percent of $CD4^{+}FoxP3^{-}CD19^{-}$ cells in the blood were TFH cells, but in the PD-$1^{-/-}$ mice this increased to ~4–5 percent (Figure 5d). This increase in PD-$1^{-/-}$ TFH cells in blood markedly contrasts with the lymph node, where PD-$1^{-/-}$ mice have similar, if not less, TFH cells compared to WT mice (Figure 1e). Importantly, TFR cells comprised ~3 percent of all FoxP3 positive cells in the blood of WT mice, but more than 7 percent of FoxP3 positive cells in the blood of PD-$1^{-/-}$ mice (Figure 5d–e). The increase in $FoxP3^{+}$ cells seems to be specific to the blood TFR subset, as the percentage of $FoxP3^{+}$ cells in the $ICOS^{+}CXCR5^{-}$ ($ICOS^{+}$) and $ICOS^{-}CXCR5^{-}$ naïve cell gates were not increased in PD-$1^{-/-}$ mice (Figure 5F). Taken together, these data indicate that both TFR and TFH cells are present in the blood of mice, and both subsets are repressed by PD-1 signals.

To investigate whether blood TFH and TFR cells have a central memory phenotype, we analyzed surface expression of CD62L and CD44. About 60% of WT and PD-$1^{-/-}$ blood TFR cells had high expression of CD62L (Figure S5). This contrasts with the greater than 90% of $ICOS^{-}CXCR5^{-}$ naïve cells that had high CD62L expression. PD-$1^{-/-}$ TFH cells had lower CD62L compared to WT TFH cells. CD44 was highly expressed on all WT and PD-$1^{-/-}$ blood TFR cells, but PD-$1^{-/-}$ blood TFR cells had slightly lower surface expression (Figure S5). Furthermore, PD-1 was expressed at lower levels on blood TFR cells than lymph node TFR cells (Figure S5). Taken together, these data indicate that blood TFR cells can have a central memory homing phenotype.

The increase in TFR cells in PD-$1^{-/-}$ mice led us to investigate which PD-1 ligand is critical for controlling lymph node and blood TFR generation. We first compared PD-L1 and PD-L2 expression on B cells and DCs present in dLNs of immunized WT mice because both B cells and dendritic cells (DCs) contribute to proper TFH differentiation and maintenance in the lymph node [1]. It is not yet clear whether B cells, DC or both are needed for TFR differentiation and/or maintenance. To study GC B cells, we immunized mice with NP-OVA subcutaneously and 12 days later compared PD-L1 and PD-L2 expression on $FAS^{+}GL7^{+}CD19^{+}$ GC B cells, as well as $CD138^{+}$ positive plasma cells (PC) from the dLN. We found that all B cell subsets expressed high levels of PD-L1, but only GC B cells expressed high levels of PD-L2 (Figure 6a). To quantify PD-L1 and PD-L2 expression on DCs, we immunized mice with NP-OVA and analyzed DC populations from the draining lymph node 3 days later. Both $CD8\alpha^{+}$ and $CD8\alpha^{-}$ DC populations expressed high levels of PD-L1 and moderate levels of PD-L2 (Figure 6b). A subpopulation of $CD8\alpha^{-}$ DCs expressed high levels of PD-L2.

To determine which ligand is important for TFH and TFR generation, we immunized WT, PD-$L1^{-/-}$ and PD-$L2^{-/-}$ mice with MOG/CFA, and analyzed TFH and TFR cells 7 days post-immunization in the draining lymph node and blood. The percentages of lymph node TFH cells in PD-$L1^{-/-}$ and PD-$L2^{-/-}$ mice were comparable to WT mice (Figure 6c) and PD-$1^{-/-}$ mice (Figure 1e). PD-$L1^{-/-}$, but not PD-$L2^{-/-}$ mice, had greater blood TFH cell numbers, which was similar to PD-$1^{-/-}$ mice (Figure 5e). TFR cells, however, were increased in the lymph nodes as well as the blood of PD-$L1^{-/-}$, but not PD-$L2^{-/-}$ mice (Figure 6d). Similar to PD-$1^{-/-}$ mice, PD-$L1^{-/-}$ mice did not exhibit any increases in non-

TFR FoxP3$^+$ effector cells within the blood (Figure 6e). These studies demonstrate that PD-L1, but not PD-L2, is responsible for controlling lymph node and blood TFR cells.

Blood TFH and TFR cells require CD28 and ICOS Signals

We further investigated the costimulatory requirements for blood TFR cells, focusing on the effects of CD28 and ICOS costimulation on CD4$^+$ICOS$^+$CXCR5$^+$FoxP3$^+$CD19$^-$ TFR populations in the blood due to the important roles of these costimulatory receptors in controlling lymph node TFH and TFR cells. CD28$^{-/-}$ mice are deficient in lymph node TFH and TFR cells [21]. ICOS$^{-/-}$ mice are deficient in lymph node TFH cells [24]. We analyzed CD28 and ICOS deficient animals for the presence of TFR cells in the lymph nodes and blood 7 days after immunization with MOG/CFA. In WT mice, there were fewer TFH and TFR cells in the blood compared to the draining lymph node (Figure 7a–b). Numbers of TFR (and TFH) cells were greatly attenuated in the blood, as well as lymph nodes, of ICOS deficient mice (Figure 7a–c). CD28 deficient mice had similar severe deficiencies in TFR and TFH cell percentages in both lymph nodes and blood (Figure 7e–f). Thus, ICOS and CD28 supply essential costimulatory signals for TFR and TFH cells in the blood as well as the lymph nodes.

PD-1 deficient blood TFR cells more potently regulate antibody production *in vivo*

We next investigated the function of blood TFR cells in humoral immune responses. Because TFH cells in human blood can function in B cell activation and antibody production *in vitro* [6, 7], we analyzed whether circulating blood TFR cells contribute to suppression of antibody production *in vivo*. To assess this, we designed transfer experiments in which we immunized >20 WT donor mice with NP-OVA subcutaneously and 8 days later sorted TFR (CD4$^+$ICOS$^+$CXCR5$^+$GITR$^+$CD19$^-$) and TFH (CD4$^+$ICOS$^+$CXCR5$^+$GITR$^-$CD19$^-$) cells from the blood (Figure 8a). We transferred these cells into CD28$^{-/-}$ or TCRα$^{-/-}$ mice because they lack both blood and lymph node TFH and TFR cells. This approach enabled us to determine if blood TFR and TFH cells could regulate humoral responses. Since the transferred blood TFH and TFR cells are the only follicular T cells in CD28$^{-/-}$ and TCRα$^{-/-}$ recipients, any responses in the draining lymph node would be due to trafficking of the blood TFR and TFH cells.

Initially, we adoptively transferred 4×10^4 TFH cells alone or together with 2×10^4 TFR cells into CD28$^{-/-}$ mice (approximately a two-fold higher ratio of TFR:TFH cells than is found in blood after immunization). We immunized recipients 1 day later with NP-OVA and analyzed NP-specific IgG titers 12 days after immunization (Figure 8a). Without blood TFH or TFR cell transfer, CD28$^{-/-}$ mice were unable to produce significant amounts of NP-specific IgG (Figure 8b). The transfer of blood TFH cells alone resulted in a substantial increase in NP-specific IgG titers. Transfer of blood TFH cells led to substantial production of IgG1, but also smaller increases in other isotypes (data not shown). Significantly, transfer of blood TFR cells along with blood TFH cells resulted in robust inhibition of NP-specific antibody production, demonstrating the potent regulatory capacity of blood TFR cells in suppressing antibody production (Figure 8b). To evaluate the impact of TFR cells on plasma cell generation, draining lymph nodes, spleens and bone marrow were harvested 24 days after immunization and plasma cells were quantified. CD138$^+$ plasma cells were absent from the lymph nodes of immunized CD28$^{-/-}$ mice (Figure 8c–d). Transfer of blood TFH cells resulted in a sizable population of plasma cells in the draining lymph node, spleen and bone marrow (Figure 8c–d). Blood TFR cells almost completely prevented plasma cell formation/survival in all organs tested.

Next we transferred blood TFH and/or TFR cells into TCRα$^{-/-}$ recipients. Transfer of 4×10^4 TFH cells resulted in high levels of NP-specific IgG and at a greater titer than an immunized

WT mouse in most experiments (Figure 8e). The robust antibody production elicited by blood TFH cells depends on the "follicular program" because transfer of total CD4 T cells from CXCR5$^{-/-}$ mice nor CD4^{+}CXCR5^{-}FoxP3^{-} naïve cells resulted in near background levels of antibody production in these experiments (Figure 8e). When blood TFR cells were transferred together with blood TFH cells, the NP-specific antibody titers were markedly reduced, demonstrating the suppressive capacity of these cells (Figure 8e). The blood TFR cells resulted in both lower plasma cell percentages (Figure 8f), as well as lower percentages of TFH cells within the lymph node (Figure 8g). When we compared the functions of blood TFH cells and draining lymph node TFH cells following transfer into TCRα$^{-/-}$ recipients, we found that blood TFH cells have an increased capacity to promote NP-specific IgG production (Figure 8h). TFR suppression of TFH cells also depends on the "follicular program" in these cells because neither blood CD25^{+}CD62L^{+} Tregs from CXCR5$^{-/-}$ mice (data not shown) nor blood CXCR5^{-} FoxP3 GFP^{+} Tregs from FoxP3 reporter mice possess the same suppressive capacity as WT blood TFR cells (Figure 8i).

Finally, we investigated the suppressive capacity of PD-1 deficient blood TFR cells *in vivo* since we have found that PD-1 deficient lymph node TFR cells more potently suppress antibody production *in vitro*. We adoptively transferred 4×10^4 blood TFH cells alone or together with 1.5×10^4 blood TFR cells from WT or PD-1 deficient mice into either CD28$^{-/-}$ or TCRα$^{-/-}$ recipients and immunized as in Figure 8a. PD-1 deficient TFR cells inhibited antibody production to a greater extent than WT TFR cells in CD28$^{-/-}$ (Figure 8j) as well as TCRα$^{-/-}$ (Figure 8k) recipients, demonstrating that they have increased suppressive capacity. Together, these data show that blood TFR cells potently inhibit antibody production *in vivo* and PD-1 deficiency results in enhanced TFR cell suppressive capacity.

Discussion

The immunoregulatory functions of the newly defined T Follicular Regulatory cell subset are only beginning to be elucidated. Relatively little is known about how these cells differentiate and function. A mechanistic understanding of TFR cell differentiation and function is needed to gain insight into how humoral immune responses are regulated by TFH and TFR cells. Although TFR cells originate from different precursors than TFH cells, TFR and TFH cells have nearly identical surface receptors. The shared expression of ICOS, CXCR5 and PD-1 by TFR and TFH cells means that functional studies of TFH cells have, in fact, examined mixtures of stimulatory TFH cells and inhibitory TFR cells. The PD-1 pathway regulates many effector arms of the immune response, however biological complexity has lead to inconsistencies regarding the role of this pathway in humoral immune responses [16–20]. In this study, we identify a new mechanism by which PD-1 regulates humoral immunity: PD-1 controls the generation and function of suppressive TFR cells. We found that lack of PD-1, or its ligand PD-L1, resulted in greater numbers of TFR cells in the draining lymph node of immunized mice. These PD-1$^{-/-}$ lymph node TFR cells expressed more *IRF4* and showed an enhanced ability to suppress antibody production. We also discovered that TFR cells are present in the blood of mice, and that PD-1 controls the numbers of blood TFR cells, as evidenced by the substantial increases in PD-1 deficient mice. Importantly, we demonstrated a functional role for blood TFH cells in promoting antibody production and blood TFR cells in suppressing antibody production *in vivo*. PD-1 deficient blood TFR cells more potently suppress antibody production compared to WT blood TFR cells. Thus, PD-1 limits the development and function of TFR cells in lymph nodes and in the circulation.

We have found that PD-1 signaling inhibits the numbers of TFR cells, but not TFH cells, in the lymph node, skewing the TFR to TFH ratio. It is possible that the greater suppressive capacity of PD-1$^{-/-}$ TFR cells, together with the increased ratio of TFR to TFH cells in

PD-1$^{-/-}$ mice, results in inhibition of PD-1$^{-/-}$ TFH cells. Alternatively, there may be alterations in PD-1$^{-/-}$ TFH cells that promote their departure from the lymph node and homing to other sites to perform effector functions. These hypotheses are not mutually exclusive. Some studies have described increases in lymph node/spleen TFH cells in PD-1 deficient mice; however the contribution of TFR cells in these studies was not assessed [16, 18, 19]. It is likely that increased TFR cells in PD-1/PD-L1 knockout mice may have contributed to the increases in TFH cells observed in these studies, and may explain, at least in part, conflicting data regarding the role of PD-1 in regulating TFH cells and germinal center reactions. For example, Kawamoto et al. described increased CD4^{+}CXCR5^{+} (TFH) cells in the Peyer's patches of PD-1 deficient mice. However, upon transfer, these cells were non-functional in supporting IgA production. Increases in TFR cells contained within the TFH gate in PD-1 deficient Peyer's patches may explain these data.

TFR cells depend on SAP, CD28 and *Bcl6* for differentiation [21, 22]. However, the pathways that limit TFR cell differentiation are less clear. To date, only the transcription factor Blimp1 has been shown to inhibit TFR cell differentiation [21]. Here we identify PD-1 as the first surface receptor that inhibits TFR cell development and function. We also show that PD-1 predominantly interacts with PD-L1, and not PD-L2, to inhibit TFR generation. Our adoptive transfer studies demonstrate a cell intrinsic role for PD-1 in TFR cell differentiation from FoxP3^{+} Treg cells. Therefore, the increase in TFR cells in PD-1 deficient mice appears to reflect increased differentiation and not maintenance. We observed a general trend for a decrease in cell cycling of CD4 PD-1$^{-/-}$ effector cells, because ICOS^{+}CXCR5^{+}FoxP3^{-} and ICOS^{+}CXCR5^{-} effector cells also had diminished Ki67 expression, at least at day 7 after immunization, which may temporally correspond to a maintenance phase. Based on these data, we hypothesize that, rather than simply inhibiting responses, the PD-1:PD-L pathway can act as a molecular switch that controls cell fate decisions in naïve CD4 T cells. Integration of signals through PD-1, the TCR and cytokine receptors may direct CD4 T cell subset differentiation. Likewise, PD-1 may limit differentiated effector T cell expansion, cytokine production and/or survival depending on how signals through the TCR, PD-1 and cytokine receptors are integrated. Thus, the PD-1 pathway can influence CD4 T cell lineage commitment in distinct ways, depending on molecular cues and the local environment. For instance, PD-L1 can promote induced Treg (iTreg) differentiation from naïve T cell precursors [10–14, 29]. However, we find that PD-1 inhibits differentiation of TFR cells. TFR cells arise from natural T regulatory cell (nTreg) precursors (shown here and previously [21]). Therefore, our studies suggest that PD-1 may have distinct roles in iTreg and nTreg differentiation. In addition genetic background may contribute to the affects of PD-1 deficiency.

Because of the recent discovery of TFR cells, there is a lack of fundamental knowledge about TFR cell biology, so we developed novel assays to analyze mechanisms by which PD-1 regulates TFR cell function. TFR cells have the potential to directly inhibit activation of naïve T cells, TFH cell function, and/or B cell activation. TFR cells might regulate TFH or B cell responses either inside the B cell follicle and/or control activation and differentiation of T cells outside the B cell follicle. Here, we present the first specific assays for TFR cell function *in vitro* and show that sorted wild type TFR cells from the lymph node are extremely potent at inhibiting antibody production, but not very effective at suppressing activation of naïve T cells. PD-1$^{-/-}$ TFR cells inhibit naïve T cell activation and attenuate antibody production *in vitro* to a greater extent than WT TFR cells. Our studies also demonstrate the dynamic control of antibody production by lymph node TFH and TFR cells. Initially, our attempts to activate B cells *in vitro* with total CD4^{+}CXCR5^{+} cells resulted in little IgG secretion. However, when we separated TFH cells from TFR cells and used these TFH cells in such experiments, we could detect robust IgG production. Of note, during an

immune response to peptide/CFA, the *in vivo* dLN TFR:TFH ratio is ~1:5. When we cultured TFR and TFH cells at this ratio, little antibody production was observed.

TFR cells tend to be present predominantly at the borders of germinal centers, which may be explained by their relatively lower expression of CXCR5 compared to TFH cells, though other chemokines also may have roles. It is possible that close proximity of TFR cells to germinal center borders enables them to interact with TFH cells as they enter. This could make TFR cells the "gate-keepers" of the germinal center, inhibiting TFH cells as they enter and gain access to B cells undergoing somatic hypermutation and class switch recombination. Furthermore, our studies suggest that the balance between TFR and TFH cells within the germinal center itself may modulate the type and extent of humoral responses. The relative roles of TFR and TFH cells also may depend on the source or strength of antigenic stimulus, cytokine milieu, and tissue microenvironment, and further work is needed to investigate these issues.

Surprisingly, we found substantial populations of TFR cells in the blood of mice. There are a number of reports describing TFH cells in the circulation of humans [6, 7] and one in mice [9]. To our knowledge, our work is the first description of TFR cells in the blood of any organism. In humans, blood TFH cells have been shown to provide B cell help for the production of antibody *in vitro.* Some studies show more efficient B cell antibody production by blood TFH cells compared to blood $CXCR5^-$ cells [6, 7] whereas other studies find no differences between blood TFH and $CXCR5^-$ cells [30]. Differences might relate to mixtures of blood TFH and TFR cells and their relative ratios in these experiments. Since most work describing blood TFH cells was done in humans, little is known about the requirements for blood TFH differentiation and function. Here we show that murine blood TFH and TFR cell generation requires signals through ICOS and CD28, two costimulatory receptors essential for controlling TFH cells in the lymph node. Previous work showed that CD28 is essential for TFR cells in lymph nodes [21]. Here we demonstrate lymph node TFR cell generation also requires ICOS signaling.

Our transfer studies show that blood TFR cells are functional and can regulate antibody production *in vivo*. To study TFH and TFR function, we transferred blood TFH cells alone or with TFR cells into $CD28^{-/-}$ or $TCR\alpha^{-/-}$ mice, which lack both blood and lymph node TFH and TFR cells. This approach allowed us to analyze TFH and TFR cell function separately from differentiation. Our transfer studies demonstrate effective and specific control of humoral responses by blood TFH and TFR cells. Blood TFR cells are extremely potent at inhibiting TFH cell mediated antibody production, even when relatively few cells are transferred. We hypothesize that blood TFR cells may represent a central memory pool that can be utilized to modulate humoral immunity, analogous to recently reported $FoxP3^+$ cells with regulatory memory to self-antigens [31] and similar to a proposed role for blood TFH cells [7]. High expression of CD62L and CD44 on blood TFR cells along with their ability to home back to lymph nodes strongly support this idea. Blood TFH cells may migrate to lymph nodes and interact with cognate B cells rapidly upon antigen exposure, whereas naïve T cells need at least two to four days to differentiate and upregulate CXCR5. Additionally, blood TFR cells homing to lymph nodes would be able to suppress early B cell responses, before dLN nTregs could fully differentiate into TFR cells.

Beyond their ability to directly suppress antibody responses, TFR cells may be instrumental in determining B cell fates and control whether an immune response generates long-lived plasma cells or memory B cells. For example, cytokines produced by TFR cells may direct GC B cell differentiation into plasma cells versus memory B cells. PD-1 and PD-1 ligand deficiency result in decreased numbers of long-lived plasma cells [16], and further work is needed to determine if this is related to enhanced $PD\text{-}1^{-/-}$ TFR cell numbers and suppressive

capacity. If TFR cells can direct B cell fates, this would have implications for rational design of vaccines. In addition, it will be interesting to determine the relative roles of TFH and TFR cells in autoimmunity. For example, PD-1 deficiency on autoimmune-prone backgrounds accelerates disease pathologies. It is possible that autoimmune-prone backgrounds may lead to inhibition of TFR differentiation and function. This information will be important for developing therapeutic strategies using TFR cells. By expanding either TFH or TFR cells from patient blood *in vitro*, it may be possible to enhance antibody responses by transferring TFH cells or to inhibit systemic autoimmunity by transferring TFR cells.

In summary, we define a new role for PD-1 in regulating immune responses, by inhibiting differentiation and function of T follicular regulatory cells in both lymph node and blood. A better understanding of TFR and TFH interactions has the potential to provide novel insights into mechanisms that regulate humoral immunity. Whether TFH and TFR cells regulate memory B cell responses is unknown and such knowledge may enable novel vaccination strategies to enhance humoral immunity. Further understanding of how PD-1 regulates humoral immunity may suggest strategies for manipulating this pathway to enhance protective immunity and long-term memory or to inhibit systemic autoimmunity.

Methods

Mice

6–10 week old mice were used for all experiments. WT C57BL/6 and TCR$\alpha^{-/-}$ mice were purchased from The Jackson Laboratory (Bar Harbor, ME). PD-$1^{-/-}$, PD-$L1^{-/-}$, and PD-$L2^{-/-}$ mice on the C57BL/6 background were generated in our laboratory [32–34]. $ICOS^{-/-}$ [35] and $CD28^{-/-}$ mice [36] were generated as described. 2D2 TCR Tg mice Foxp3-IRES-GFP knockin mice (Foxp3.GFP; [37] were generated in our laboratory by crossing 2D2 TCR Tg mice [38] with Foxp3.GFP reporter mice. All mice were used according to the Harvard Medical School Standing Committee on Animals and National Institutes of Animal Healthcare Guidelines. Animal protocols were approved by the Harvard Medical School Standing Committee on Animals.

Immunizations

For MOG 35–55 immunizations (referred to as “MOG/CFA”), mice were injected subcutaneously with 100μg of MOG 35–55 (UCLA Biopolymers Facility) emulsified in a 1:1 emulsion of H37RA CFA (Sigma) on the mouse flanks. Seven days later mice were euthanized and inguinal lymph nodes (dLN) and/or spleen were harvested for flow cytometric analyses. Blood was collected via cardiac puncture with a 1cc syringe and immune cells were isolated by sucrose density centrifugation using Lymphocyte Separation Media (LSM). For NP-OVA immunizations, 100μg NP_{18}-OVA (Biosearch Technologies) was used in a 1:1 H37RA CFA emulsion and injected similarly as MOG/CFA.

ELISA

For *in vitro* quantitation of antibody production, supernatants were taken from cultures and total IgG was quantified using pan-IgG capture antibody (Southern Biotech) and alkaline phosphatase conjugated pan-IgG detection antibody (Southern Biotech). To assess *in vivo* antibody production, sera were collected from mice at indicated time points. NP-specific antibody titers were measured by coating ELISA plates with NP_{16}-BSA (Biosearch Technologies), and incubating serum for 1hr followed by alkaline phosphatase-conjugated IgG detection antibodies. A standard curve was generated using antibody from an NP-specific IgG1 hybridoma (a kind gift of Dr. Michael Carroll). This standard curve was used to approximate all IgG subtype antibody levels in the linear range of detection using a Spectramax Elisa plate reader (Molecular Devices).

Flow Cytometry

Cells from lymphoid organs were isolated and resuspended in staining buffer (PBS containing 1% fetal calf serum and 2mM EDTA) and stained with directly labeled antibodies from Biolegend against CD4 (RM4-5), ICOS (15F9), CD19 (6D5), PD-1 (RMP1-30), PD-L1 (10F.9G2), CD69 (H1.2F3), from eBioscience against FoxP3 (FJK-16S), Bcl6 (mGI191E), and from BD bioscience against FAS (Jo2), GL7, Ki67 (B56). For CXCR5 staining, biotinylated anti-CXCR5 (2G8, BD Biosciences) was used followed by streptavidin-brilliant violet 421 (Biolegend). For intracellular staining, the FoxP3 fix/perm kit was used (eBioscience) after surface staining was accomplished. All flow cytometry was analyzed with an LSR II (BD biosciences) using standard filter sets.

Confocal Microscopy

Draining lymph nodes were embedded in OCT and 8μm sections were cut, fixed with 4% paraformaldehyde, and stained before imaging on a Zeiss LSM 510 confocal microscope by acquiring z-stacks of 0.5um with a 40x oil objective. Germinal center quantitation was calculated by drawing outlines around $GL7^{+}IgD^{-}$ areas present within the B cell zone. FoxP3 quantitation was performed by determining germinal center zones and scrolling through z-stack images to identify large FoxP3 positive spots. Axiovision (Zeiss) software was used to measure distances from germinal center borders. For micrograph panels, single z slices were linearly contrasted and merged images were made in Adobe photoshop.

Quantitative PCR

Q-PCR was performed using standard TaqMAN probes (Applied Biosystems) and an ABI FAST9500 QPCR machine according to the manufacturer's instructions. mRNA levels were normalized to HPRT or β2M, and the $2^{-\text{deltadeltaCT}}$ method was used to quantitate mRNA. Each bar graph represents mean values from more than three individual experiments consisting of cells sorted from 5–10 pooled mice.

In vitro Suppression Assay

Cell populations were sorted to 99% purity on an Aria II flow cytometer. For TFR suppression assays, sorted cells were counted on an Accuri cytometer (BD biosciences) by gating live cells only, and 1×10^{5} $GL7^{-}$ B cells from dLNs of WT mice immunized with MOG/CFA 7 days previously, 1×10^{5} CFSE labeled $CD4^{+}CD62L^{+}FoxP3^{-}$ T responder cells from unimmunized WT FoxP3 GFP reporter mice, and 1×10^{5} TFR cells from the draining dLN of 10 pooled mice immunized with MOG/CFA 7 days previously were plated with 2μg/ml soluble anti-CD3 (2C11, BioXcell) and 5μg/ml anti-IgM (Jackson Immunoresearch). After 3 days, cells were harvested and stained for CD4 and CD19. T cell responders were identified as CFSE positive, and percent divided was gated as the percent of cells with CFSE diluted compared to unstimulated T responders.

Adoptive Transfers

For blood TFH/TFR adoptive transfers, 20 to 30 WT mice were immunized with NP-OVA subcutaneously as described above, and 8 days later blood was collected by cardiac puncture. TFH and TFR cells were sorted as described. 4×10^{4} blood TFH cells alone or together with 2×10^{4} blood TFR cells were transferred into $CD28^{-/-}$ or $TCR\alpha^{-/-}$ mice unless specified otherwise. These recipient mice were immunized with NP-OVA as described above. Serum and organs were harvested at indicated times and analyzed by ELISA or flow cytometry.

Statistical Analysis

Unpaired Student's t test was used for all comparisons, data represented as mean +/− SD or SE are shown. P values < 0.05 were considered statistically significant. * P<0.05, ** P<0.005, *** P<0.0005.

Supplementary Material

Refer to Web version on PubMed Central for supplementary material.

Acknowledgments

We thank Robert Ortega, Caroline Armet, Flor Gonzalez and Dr. Dan Brown for outstanding technical assistance with these studies, Dr. Gordon Freeman for his thoughtful comments on the manuscript, and Dr. Michael Carroll for the gift of a mouse anti-NP standard. This work was supported by NIH grants T32 AI070085 to P.T.S., and R01 AI40614 and P01 78897 to A.H.S.

References

1. Crotty S. Follicular helper CD4 T cells (TFH). Annu Rev Immunol. 2011; 29:621–663. [PubMed: 21314428]
2. Johnston RJ, et al. Bcl6 and Blimp-1 are reciprocal and antagonistic regulators of T follicular helper cell differentiation. Science. 2009; 325:1006–1010. [PubMed: 19608860]
3. Nurieva RI, et al. Bcl6 mediates the development of T follicular helper cells. Science. 2009; 325:1001–1005. [PubMed: 19628815]
4. Choi YS, et al. ICOS receptor instructs T follicular helper cell versus effector cell differentiation via induction of the transcriptional repressor Bcl6. Immunity. 2011; 34:932–946. [PubMed: 21636296]
5. Nurieva RI, et al. Generation of T follicular helper cells is mediated by interleukin-21 but independent of T helper 1, 2, or 17 cell lineages. Immunity. 2008; 29:138–149. [PubMed: 18599325]
6. Morita R, et al. Human blood CXCR5(+)CD4(+) T cells are counterparts of T follicular cells and contain specific subsets that differentially support antibody secretion. Immunity. 2011; 34:108–121. [PubMed: 21215658]
7. Schaerli P, et al. CXC chemokine receptor 5 expression defines follicular homing T cells with B cell helper function. J Exp Med. 2000; 192:1553–1562. [PubMed: 11104798]
8. Saito R, et al. Altered expression of chemokine receptor CXCR5 on T cells of myasthenia gravis patients. Journal of neuroimmunology. 2005; 170:172–178. [PubMed: 16214223]
9. Simpson N, et al. Expansion of circulating T cells resembling follicular helper T cells is a fixed phenotype that identifies a subset of severe systemic lupus erythematosus. Arthritis and rheumatism. 2010; 62:234–244. [PubMed: 20039395]
10. Polanczyk MJ, Hopke C, Vandenbark AA, Offner H. Treg suppressive activity involves estrogen-dependent expression of programmed death-1 (PD-1). Int Immunol. 2007; 19:337–343. [PubMed: 17267414]
11. Wang L, et al. Programmed death 1 ligand signaling regulates the generation of adaptive Foxp3+CD4+ regulatory T cells. Proc Natl Acad Sci U S A. 2008; 105:9331–9336. [PubMed: 18599457]
12. Francisco LM, et al. PD-L1 regulates the development, maintenance, and function of induced regulatory T cells. J Exp Med. 2009; 206:3015–3029. [PubMed: 20008522]
13. Wang C, Li Y, Proctor TM, Vandenbark AA, Offner H. Down-modulation of programmed death 1 alters regulatory T cells and promotes experimental autoimmune encephalomyelitis. Journal of neuroscience research. 2010; 88:7–15. [PubMed: 19642196]
14. Amarnath S, et al. The PDL1-PD1 axis converts human TH1 cells into regulatory T cells. Science translational medicine. 2011; 3:111ra120.
15. Francisco LM, Sage PT, Sharpe AH. The PD-1 pathway in tolerance and autoimmunity. Immunol Rev. 2009; 236:219–242. [PubMed: 20636820]

16. Good-Jacobson KL, et al. PD-1 regulates germinal center B cell survival and the formation and affinity of long-lived plasma cells. Nature immunology. 2010; 11:535–542. [PubMed: 20453843]
17. Hamel KM, et al. B7-H1 expression on non-B and non-T cells promotes distinct effects on T- and B-cell responses in autoimmune arthritis. Eur J Immunol. 2010; 40:3117–3127. [PubMed: 21061440]
18. Kawamoto S, et al. The inhibitory receptor PD-1 regulates IgA selection and bacterial composition in the gut. Science. 2012; 336:485–489. [PubMed: 22539724]
19. Hams E, et al. Blockade of B7-H1 (programmed death ligand 1) enhances humoral immunity by positively regulating the generation of T follicular helper cells. J Immunol. 2011; 186:5648–5655. [PubMed: 21490158]
20. Velu V, et al. Enhancing SIV-specific immunity in vivo by PD-1 blockade. Nature. 2009; 458:206–210. [PubMed: 19078956]
21. Linterman MA, et al. Foxp3+ follicular regulatory T cells control the germinal center response. Nat Med. 2011; 17:975–982. [PubMed: 21785433]
22. Chung Y, et al. Follicular regulatory T cells expressing Foxp3 and Bcl-6 suppress germinal center reactions. Nat Med. 2011; 17:983–988. [PubMed: 21785430]
23. Wollenberg I, et al. Regulation of the germinal center reaction by Foxp3+ follicular regulatory T cells. J Immunol. 2011; 187:4553–4560. [PubMed: 21984700]
24. Bauquet AT, et al. The costimulatory molecule ICOS regulates the expression of c-Maf and IL-21 in the development of follicular T helper cells and TH-17 cells. Nature immunology. 2009; 10:167–175. [PubMed: 19098919]
25. Fife BT, et al. Interactions between PD-1 and PD-L1 promote tolerance by blocking the TCR-induced stop signal. Nature immunology. 2009; 10:1185–1192. [PubMed: 19783989]
26. Cretney E, et al. The transcription factors Blimp-1 and IRF4 jointly control the differentiation and function of effector regulatory T cells. Nature immunology. 2011; 12:304–311. [PubMed: 21378976]
27. Martins GA, et al. Transcriptional repressor Blimp-1 regulates T cell homeostasis and function. Nature immunology. 2006; 7:457–465. [PubMed: 16565721]
28. Zhou L, et al. TGF-beta-induced Foxp3 inhibits T(H)17 cell differentiation by antagonizing RORgammat function. Nature. 2008; 453:236–240. [PubMed: 18368049]
29. Beswick EJ, Pinchuk IV, Das S, Powell DW, Reyes VE. Expression of the programmed death ligand 1, B7-H1, on gastric epithelial cells after Helicobacter pylori exposure promotes development of CD4+ CD25+ FoxP3+ regulatory T cells. Infect Immun. 2007; 75:4334–4341. [PubMed: 17562772]
30. Kim CH, et al. Subspecialization of CXCR5+ T cells: B helper activity is focused in a germinal center-localized subset of CXCR5+ T cells. J Exp Med. 2001; 193:1373–1381. [PubMed: 11413192]
31. Rosenblum MD, et al. Response to self antigen imprints regulatory memory in tissues. Nature. 2011; 480:538–542. [PubMed: 22121024]
32. Keir ME, Freeman GJ, Sharpe A. PD-1 regulates self-reactive CD8+ T cell responses to antigen in lymph nodes and tissues. Journal of Immunology. 2007; 179:5064–5070.
33. Latchman YE, et al. PD-L1-deficient mice show that PD-L1 on T cells, antigen-presenting cells, and host tissues negatively regulates T cells. Proc Natl Acad Sci U S A. 2004; 101:10691–10696. [PubMed: 15249675]
34. Keir ME, et al. Tissue expression of PD-L1 mediates peripheral T cell tolerance. J Exp Med. 2006; 203:883–895. [PubMed: 16606670]
35. McAdam AJ, et al. ICOS is critical for CD40-mediated antibody class switching. Nature. 2001; 409:102–105. [PubMed: 11343122]
36. Shahinian A, et al. Differential T cell costimulatory requirements in CD28-deficient mice. Science. 1993; 261:609–612. [PubMed: 7688139]
37. Bettelli E, et al. Reciprocal developmental pathways for the generation of pathogenic effector TH17 and regulatory T cells. Nature. 2006; 441:235–238. [PubMed: 16648838]

38. Bettelli E, et al. Myelin oligodendrocyte glycoprotein-specific T cell receptor transgenic mice develop spontaneous autoimmune optic neuritis. J Exp Med. 2003; 197:1073–1081. [PubMed: 12732654]

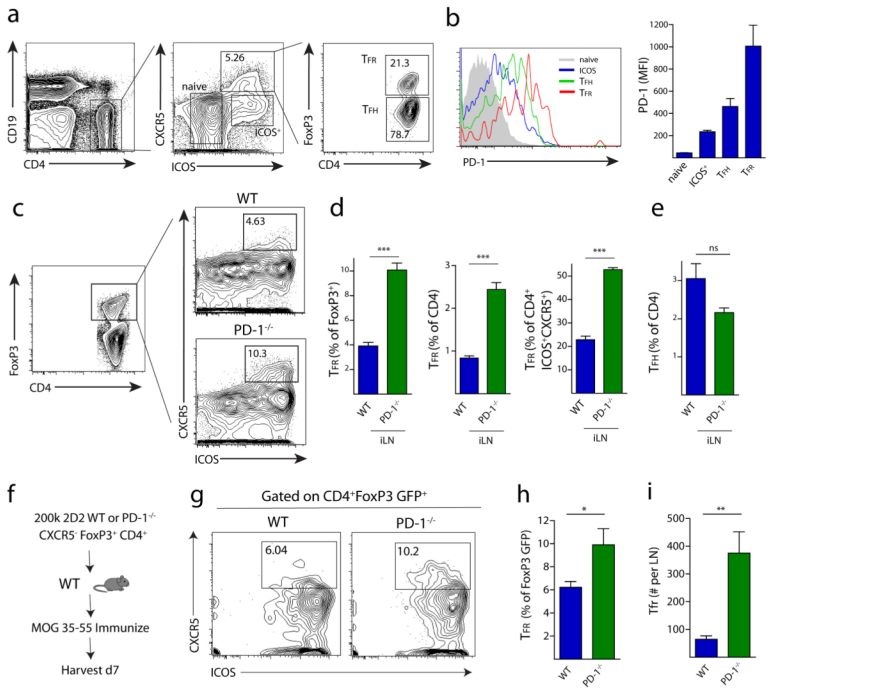

Figure 1.

PD-1 signaling in FoxP3 Tregs limits the generation of T follicular regulatory cells. (**a**) Quantitation of TFR cells. WT mice were immunized with MOG/CFA and 7 days later draining lymph nodes were isolated and immediately stained for $CD4^+FoxP3^+ICOS^+CXCR5^+CD19^-$ T follicular regulatory cells (TFR), $CD4^+FoxP3^-ICOS^+CXCR5^+CD19^-$ T follicular helper cells (TFH), $CD4^+ICOS^-CXCR5^-CD19^-$ cells (naive) or $CD4^+ICOS^+CXCR5^-CD19^-$ cells (ICOS+). Numbers indicate percentages of cells located within each gate. (**b**) PD-1 expression by flow cytometry on WT naive, ICOS+, TFR and TFH cells. Populations were gated as in (**a**). (**c**) Gating of TFR cells from total $FoxP3^+$ cells in WT and PD-$1^{-/-}$ mice immunized with MOG/CFA and analyzed 7 days later and stained as in **(a)**. (**d**) Quantitation of WT or PD-$1^{-/-}$ TFR cells gated in (**c**) and expressed as a percentage of $CD4^+FoxP3^+$ (left), percentage of total CD4 T cells (middle), or percentage of $CD4^+ICOS^+CXCR5^+CD19^-$ gate (right). (**e**) Quantitation of TFH cells as a percentage of total CD4 T cells. Data represent means of 5 mice per group. All error bars indicate standard error. (**f**) PD-1 on $FoxP3^+$ cells has a cell-intrinsic role in inhibiting TFR differentiation *in vivo*. Schematic design of a transfer assay in which 2D2 TCR transgenic $CD4^+FoxP3^+CXCR5^-$ non-TFR Tregs were transferred into WT mice which were subsequently immunized with MOG/CFA. Draining lymph nodes were harvested 7 days later and analyzed for TFR cells. (**g**) Representative gating of TFR cells from transfer experiments described in (**f**). (**h–i**) Quantitation of TFR cells from transfer experiments expressed as a percentage of FoxP3 GFP^+ cells present on day 7 post immunization (**h**) or total cell number (**i**) per lymph node. All data are representative of at least two independent experiments with at least 5 mice per group. All error bars indicate standard error. * $P<0.05$, ** $P<0.005$

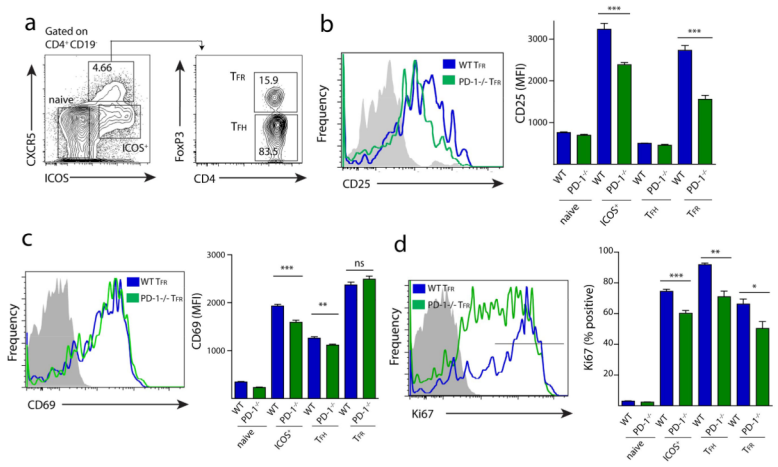

Figure 2.

PD-1 deficient TFR cells have altered expression of activation markers. (**a)** TFR cell gating strategy. WT or PD-1$^{-/-}$ mice were immunized with MOG/CFA and draining lymph nodes were harvested 7 days later. (**b**) CD25 expression on WT and PD-1$^{-/-}$ CD4 subsets gated as in (**a**). Overlay histograms of WT and PD-1$^{-/-}$ TFR cells (left) and mean fluorescence intensity (MFI) in CD4 subsets gated as in (**a**) (right). Data represent means of 5 mice per group. (**c**) CD69 expression on WT and PD-1$^{-/-}$ CD4 subsets gated as in (**a**). Overlay histograms of WT and PD-1$^{-/-}$ TFR cells (left) and MFI (right). Data represent means of 5 mice per group. (**d**) Intracellular staining of cell cycle marker Ki67 in populations as in (**a**). Overlay histograms of WT and PD-1$^{-/-}$ TFR cells (left) and percent Ki67 high (right) in CD4 subsets gated as in (**a**). Ki67 high was defined as the highest intensity peak on WT TFR cells and is denoted by a black bar on the histogram. Data represent means of 5 mice per group. All data are representative of at least two independent experiments. All error bars indicate standard error. * P<0.05, ** P<0.005, *** P<0.0005.

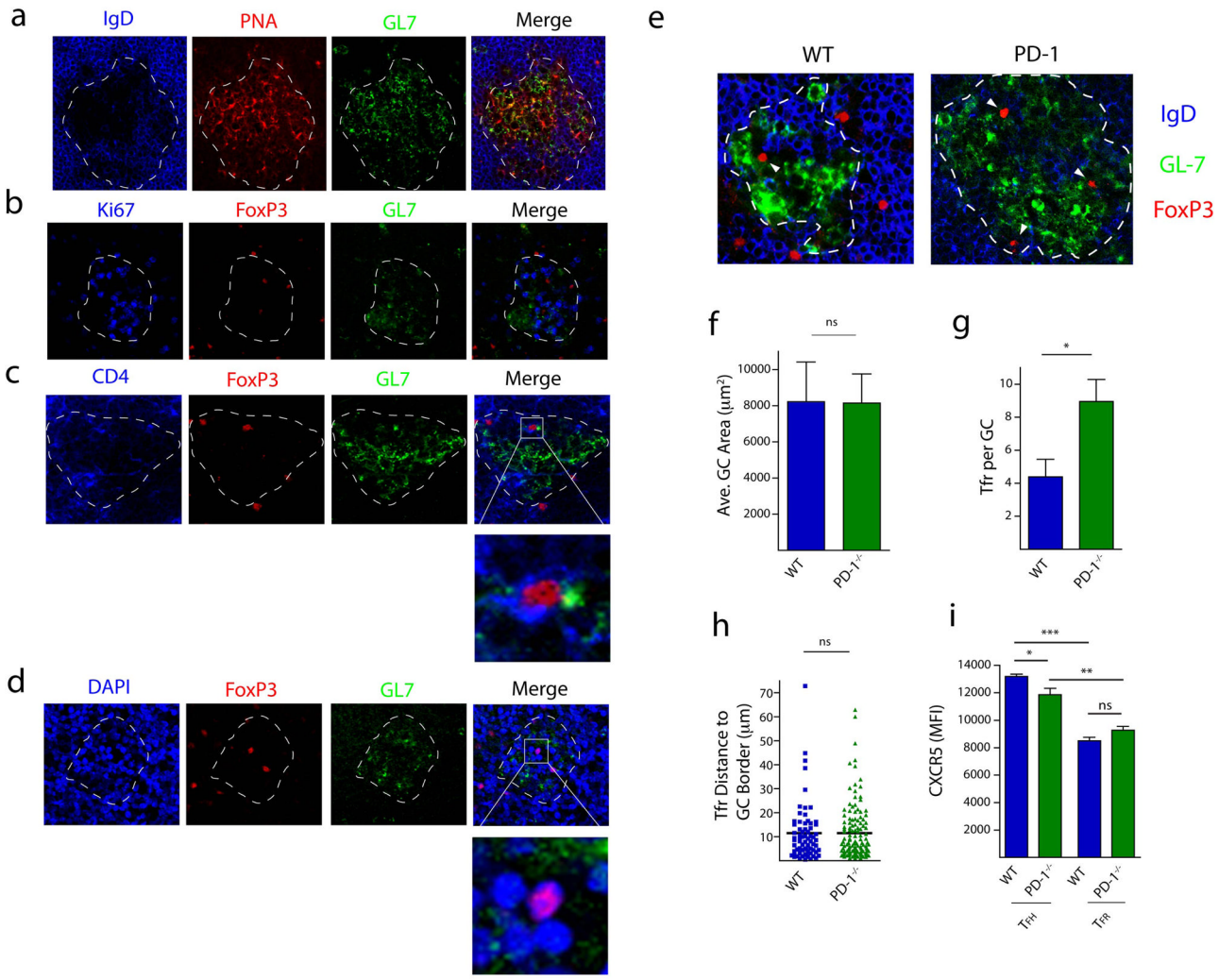

Figure 3.

PD-1 deficient TFR cells are capable of homing to germinal centers (GCs). (**a**) Micrographs of draining lymph node sections from WT mice immunized with MOG/CFA and harvested 7 days later. Sections were cut and stained for GL-7 (green), PNA (red) and IgD (blue). GCs were identified by PNA and GL7 positive, but IgD negative, staining. GCs are indicated with a white dotted line. (**b**) Ki67 staining in GCs. Sections were stained for the cell cycle marker Ki67 (blue), FoxP3 (red) and GL7 (green). (**c**) Colocalization of CD4 and FoxP3. Sections were stained for CD4 (blue), FoxP3 (red) and GL7 (green). Box indicates magnification highlighting CD4 positive staining on $FoxP3^+$ cells (**d**) Colocalization of FoxP3 in the nucleus. Sections were stained with the nuclear stain DAPI (blue), FoxP3 (red) and GL7 (green). Box indicates magnification highlighting FoxP3 protein within DAPI positive nuclei. (**e**) Comparison of $FoxP3^+$ TFR cells in germinal centers of WT and PD-$1^{-/-}$ mice. Representative GC staining in WT and PD-$1^{-/-}$ lymph nodes 7 days after immunization with MOG/CFA. (**f**) Average GC area was determined by calculating the area within the dotted lines according to materials and methods. Data represent mean area per lymph node of 5 individual mice. (**g**) Numbers of $FoxP3^+$ cells contained within GCs. Data represent mean per GC from 5 pooled mice. (**h**) Quantitation of the distance of each $FoxP3^+$ cell to the GC border. The distance for each $FoxP3^+$ cell in (**e**) from the GC borders (dotted line in (**e**)) was calculated as described in materials and methods. (**i**) CXCR5 expression was

quantified on WT and PD-1$^{-/-}$ CD4^{+}ICOS^{+}CXCR5^{+}FoxP3^{-}CD19^{-} TFH and CD4^{+}ICOS^{+}CXCR5^{+}FoxP3^{+}CD19^{-} TFR cells by flow cytometry 7 days after MOG/CFA immunization. Data represent means of 5 mice per group. * P<0.05, ** P<0.005, *** P<0.0005.

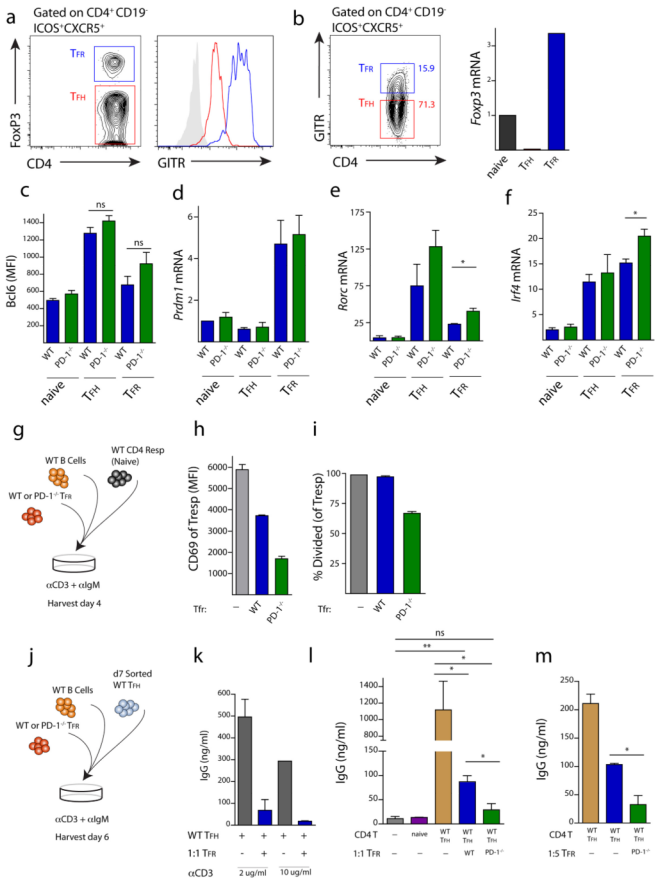

Figure 4.

PD-1 deficient TFR cells have enhanced regulatory capacity. (**a**) TFR cells express high levels of GITR. WT mice were immunized with MOG/CFA and 7 days later lymph node cells were isolated and expression of GITR on TFR ($CD4^+FoxP3^+ICOS^+CXCR5^+CD19^-$, blue) and TFH ($CD4^+FoxP3^-ICOS^+CXCR5^+CD19^-$, red) was quantified as shown by histogram overlays. (**b**) Expression of FoxP3 mRNA in sorted TFR ($CD4^+GITR^+ICOS^+CXCR5^+CD19^-$), TFH ($CD4^+GITR^-ICOS^+CXCR5^+CD19^-$) and naive ($CD4^+ICOS^-CXCR5^-CD19^-$) cells. Data represent fold change in mRNA normalized to *Hprt.* (**c**) Bcl6 expression analyzed by intracellular flow cytometry on TFH and TFR cells from WT (blue) and PD-$1^{-/-}$ (green) mice. (**d–f**) mRNA expression of (**d**) blimp-1/*Prdm1* (**e**) *Rorc* and (**f**) *Irf4* from sorted WT (blue) and PD-$1^{-/-}$ (green) TFR and TFH cells and in CD4-$ICOS^-CXCR5^-$ (naive) cells quantified by qPCR analysis. Data represent means from at least three separate experiments in which cells were sorted from lymph nodes of 10 pooled mice. (**g**) Design of assay to analyze capacity of TFR cells to inhibit activation of naïve CD4 T cells. WT and PD-$1^{-/-}$ mice were immunized with MOG/CFA and TFR cells were sorted from draining lymph nodes and plated 1:1:1 with CFSE-labeled CD4 naïve WT ($CD4^+CD62L^+FoxP3^-$) responder cells and WT $GL7^-B220^+$ B cells from MOG/CFA immunized mice along with anti-CD3 and anti-IgM for 4 days. 3 days later samples were analyzed by flow cytometry. (**h**) PD-$1^{-/-}$ TFR cells suppress activation of naïve T cells to a greater extent than WT TFR cells. T responders from suppression assays from **(g)** were analyzed for CD69 expression (**h**) and proliferation (**i**) by measuring CFSE dilution. % divided indicates percent of cells that have gone through at least one division. (**j**) *In vitro* IgG suppression assay design. TFR cells sorted as in (**g**) were plated in a 1:1:1 ratio of TFR ($CD4^+ICOS^+CXCR5^+GITR^+CD19^-$), TFH ($CD4^+ICOS^+CXCR5^+GITR^-CD19^-$), and B

(GL-7^{-}B220^{+}) cells from draining lymph nodes of MOG/CFA immunized mice in the presence of anti-CD3 and anti-IgM for 6 days. Total IgG was measured by ELISA from supernatants. (**k**) Suppression assay using two concentrations of anti-CD3. (**l**) PD-1 deficient TFR cells suppress IgG production to a greater extent than WT TFR cells at a 1:1 TFR:TFH ratio. Naive (CD4^{+}ICOS^{-}CXCR5^{-}CD19^{-}) cells from immunized mice were included as controls. (**m**) PD-1 deficient TFR cells suppress IgG production to a greater extent than WT TFR cells at a 1:5 TFR:TFH ratio. Data indicates means +/− standard error of replicate wells and is representative of at least two experiments (**h–m**). * P<0.05, ** P<0.005, *** P<0.0005.

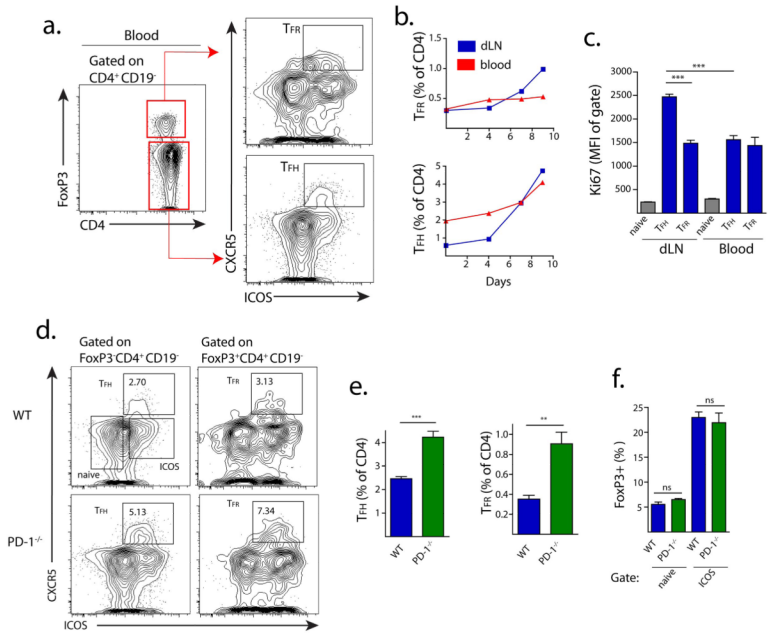

Figure 5.

PD-1 controls circulating blood TFR cells. (**a**) Gating strategy to identify circulating TFH and TFR cells from blood. WT mice were immunized with MOG/CFA and blood was collected 7 days later by cardiac puncture. TFH and TFR populations were gated as shown. (**b**) Quantitation of blood TFH and TFR cells following MOG/CFA immunization. Mice were immunized as in **(a)** and sacrificed on the indicated days. Blood was collected and cells stained and gated as in **(a)**. (**c**) Ki67 expression in blood and lymph node TFH, TFR and naïve ($CD4^+ICOS^-CXCR5^-$) cells 7 days after MOG/CFA immunization. (**d–f**) Comparison of blood TFH and TFR cells in WT and PD-$1^{-/-}$ mice immunized as in **(a)** and harvested 7 days after immunization**. (d)** Blood TFH cells are shown gated on $FoxP3^-CD4^+CD19^-$ (left) and TFR cells are shown gated on $FoxP3^+CD4^+CD19^-$ (right). (**e**) Quantitation of blood TFH and TFR cells from immunized WT and PD-$1^{-/-}$ mice gated as in **(d)** and expressed as a percent of $CD4^+CD19^-$ cells. (**f**) Quantitation of $CXCR5^-$ $FoxP3^+$ cells from immunized WT and PD-$1^{-/-}$ mice, expressed as a percentage of $CXCR5^-$ $CD4^+$ cells. All data indicates means +/− standard error of 5 mice and is representative of at least two independent experiments. * P<0.05, ** P<0.005, *** P<0.0005.

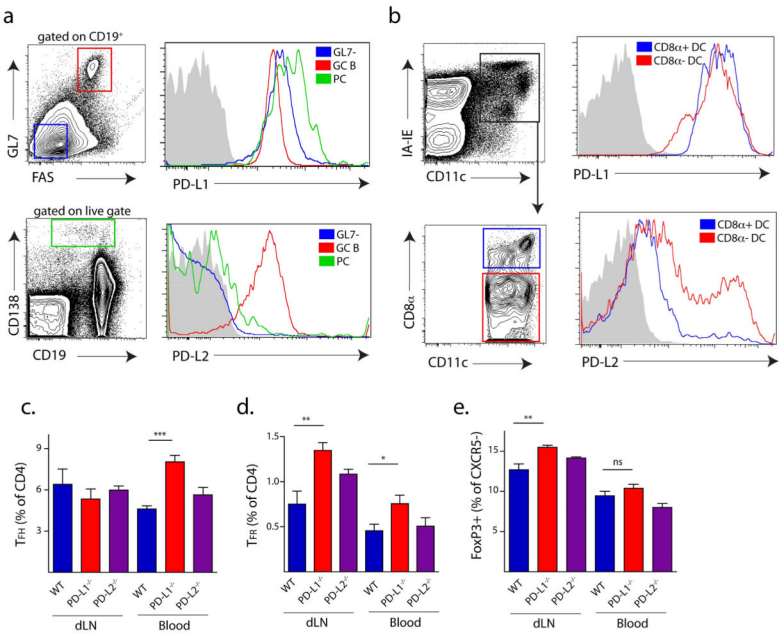

Figure 6.

PD-L1 but not PD-L2 controls blood TFR cells. (**a**) PD-L1 and PD-L2 expression on B cell subsets. WT mice were immunized with NP-OVA subcutaneously and 12 days later germinal center B (GC B), GL7^{-}, and plasma cells (PC) from draining lymph nodes were analyzed for PD-L1 (top) and PD-L2 (bottom) expression. (**b**) PD-L1 and PD-L2 expression on dendritic cells (DC). WT mice were immunized with NP-OVA and 3 days later CD8α^{+} DC and CD8α^{-} DC subsets from draining lymph nodes were analyzed for PD-L1 (top) and PD-L2 (bottom) expression. (**c**) Lymph node and blood TFH and TFR cells in PD-1 ligand deficient mice. WT, PD-L1$^{-/-}$ and PD-L2$^{-/-}$ mice were immunized with MOG/CFA, and 7 days later draining lymph nodes and blood were harvested and analyzed for TFH (**c**), TFR (**d**) and CXCR5^{-} FoxP3^{+} (**e**) CD4 T cells. Data represent means of 5 mice per group. All data are representative of at least two independent experiments. * P<0.05, ** P<0.005, *** P<0.0005.

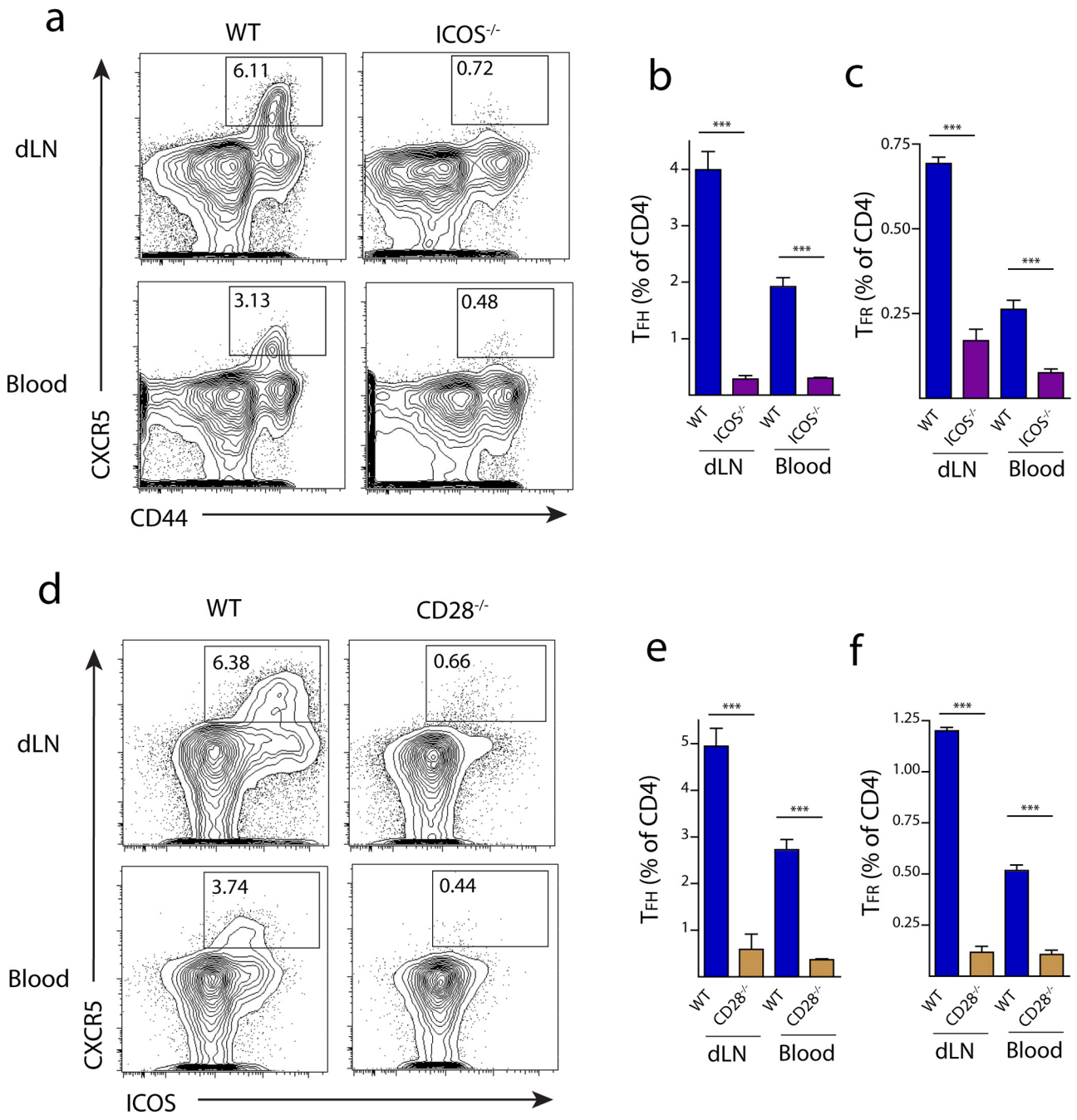

Figure 7.

Blood TFR cells require ICOS and CD28 costimulation. (**a**) TFH and TFR gating in WT and ICOS$^{-/-}$ mice. Mice were immunized with MOG/CFA and 7 days later draining lymph nodes (dLN) and blood were harvested. TFH cells were gated as CD4^{+}CD44^{+}CXCR5^{+}FoxP3^{-}CD19^{-}, and TFR cells as CD4^{+}CD44^{+}CXCR5^{+}FoxP3^{+}CD19^{-} cells. TFH (**b**) and TFR (**c**) quantitation in lymph nodes (dLN) and blood of WT and ICOS$^{-/-}$ mice as in **(a)**. (**d**) TFH and TFR gating strategy in WT and CD28$^{-/-}$ mice. Mice were immunized as in **(a)** and TFH cells were gated as CD4^{+}ICOS^{+}CXCR5^{+}FoxP3^{-}CD19^{-} and TFR cells as CD4^{+}ICOS^{+}CXCR5^{+}FoxP3^{+}CD19^{-}. TFH (**e**) and TFR (**f**) quantitation in

lymph nodes and blood of WT and CD28$^{-/-}$ mice gated as in **(d)**. All data are representative of at least two independent experiments. * P<0.05, ** P<0.005, *** P<0.0005.

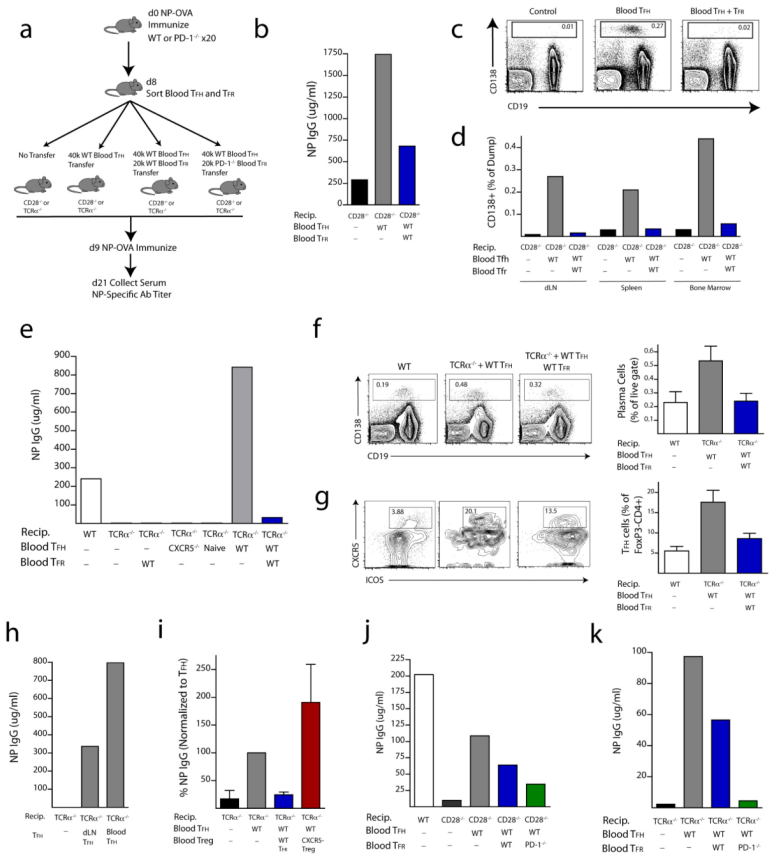

Figure 8.

PD-1 deficient blood TFR cells more potently regulate antibody production *in vivo.* (**a**) Experimental strategy to assess blood TFH and TFR cell function by transfer of blood TFH and/or TFR cells into mice that lack both lymph node and blood TFH/TFR cells. Blood TFH and/or TFR cells were isolated from 20 pooled mice immunized with NP-OVA 8 days previously and $CD4^+CXCR5^+GITR^-CD19^-$ TFH and $CD4^+CXCR5^+GITR^+CD19^-$ TFR cells were purified by cell sorting; recipient $CD28^{-/-}$ or $TCR\alpha^{-/-}$ mice received either no cells, 4×10^4 TFH cells, or 4×10^4 TFH plus 2×10^4 TFR cells. One day later recipients were immunized with NP-OVA. 12 days later sera were collected and NP-specific antibody titers quantified by ELISA. (**b**) WT blood TFR cells potently suppress antibody production. NP-specific antibody titers from experiments as in **(a)** in which WT TFH or WT TFH plus WT TFR cells were transferred into $CD28^{-/-}$ recipients. (**c**) $CD138^+$ plasma cell percentages in draining lymph nodes of $CD28^{-/-}$ recipients following no transfer (Control), Blood TFH transfer (Blood TFH) or Blood TFH plus TFR cell transfer (Blood TFH + TFR) 24 days after immunization. Cells are gated as a percentage of $CD11b^-CD11c^-Ly6c^-$ (dump) cells. (**d**) Quantitation of CD138 plasma cells as gated in (**c**) in draining lymph node, spleen and bone marrow. (**e**) Blood TFH and/or TFR Transfer into $TCR\alpha^{-/-}$ recipients using experimental design as in **(a)**. Comparison of NP-specific antibody titers in (1) WT control mice, (2) $TCR\alpha^{-/-}$ recipients $^{-/-}$ recipients given WT blood T $^{-/-}$ given no cells, (3) TCRα FR cells alone, (4) TCRα recipients given total blood CD4 T cells from $CXCR5^{-/-}$ mice immunized with NP-OVA 8 days previously, (5) $TCR\alpha^{-/-}$ recipients given blood $CD4^+FoxP3^-$ cells from unimmunized FoxP3-GFP mice, (6) $TCR\alpha^{-/-}$ recipients given WT blood TFH cells, and (7) $TCR\alpha^{-/-}$ recipients given WT blood TFH cells plus TFR cells. NP specific IgG levels were determined by ELISA. (**f**) $CD138^+$ plasma cells from the spleen (gated as a percent of live cells) and (**g**) $CD4^+FoxP3^-$ TFH cells from the draining lymph

node pre-gated on $CD4^{+}FoxP3^{-}$ were quantified from experiments in (**e**) 12 days after secondary immunization. Error bars indicate standard error of at least three separate experiments. (**h**) Blood TFH cells can have an enhanced ability to stimulate antigen-specific antibody production compared to lymph node TFH cells. Blood TFH cells and draining lymph node TFH cells were isolated from WT mice immunized with NP-OVA 8 days previously and 4×10^{6} cells were transferred into $TCR\alpha^{-/-}$ mice and immunized as in (**e**). (**i**) Blood TFR cell suppression is aided by the follicular program. Blood TFH cells were transferred to $TCR\alpha^{-/-}$ mice along with blood CXCR5− FoxP3 GFP^{+} cells from FoxP3 reporter mice or blood TFR cells. Antibody titers were quantified 12 days after NP-OVA immunization and NP IgG levels are expressed as a percent of TFH transfer group. Data indicate standard error of at least three independent experiments. (**j–k**) PD-1 deficient blood TFR cells more potently suppress antibody production *in vivo* compared to WT TFR cells. 4×10^{4} WT blood TFH and 1.5×10^{4} WT or PD-1 deficient blood TFR cells from mice immunized with NP-OVA 8 days previously were transferred into $CD28^{-/-}$ mice (**j**) or $TCR\alpha^{-/-}$ mice (**k**). Recipient mice were immunized with NP-OVA, and NP specific antibody titers were measured from serum 12 days later. Data are representative of two independent experiments.